Journal of Circuits, Systems, and Computers, Vol. 11, No. 1 (2002) 1–16

A SYSTEMATIC PROCEDURE FOR SYNCHRONIZING HYPERCHAOS VIA OBSERVER DESIGN

GIUSEPPE GRASSI*

Dipartimento di Ingegneria dell'Innovazione,
Università di Lecce, 73100 Lecce, Italy
giuseppe.grassi@unile.it

SAVERIO MASCOLO

Dipartimento di Elettrotecnica ed Elettronica,
Politecnico di Bari, 70125 Bari, Italy
mascolo@poliba.it

Received 19 February 1999
Revised 4 December 2000

In this Letter a systematic procedure for synchronizing different classes of hyperchaotic systems is illustrated. The approach can be applied to dynamic systems with one or more nonlinear elements as well as to time delay systems. The method is rigorous and systematic. Namely, if a structural property related to the drive system is satisfied, it is easy to design the synchronizing signal and the response system, which is chosen in the observer form. The technique is successfully applied to a recent example of 8th order circuit, to a cell equation in delayed Cellular Neural Networks and to an example of high dimensional system, which consists of five identical coupled Chua's circuits forming a ring. Simulation results are reported to show the performances of the technique.

1. Introduction

The goal of synchronization is to design a coupling between two chaotic systems, called drive system and response system, so that their dynamics become identical after a transient time.[1–6] The coupling is implemented via a synchronizing signal, which is generated by the drive system. Most of the methods developed in literature concerns the synchronization of low dimensional systems, characterized by only one positive Lyapunov exponent,[1,2] even though the synchronization of hyperchaotic systems (that is, systems with more than one positive Lyapunov exponent) has recently become a field of active research.[3–6]

It should be noted that, given the drive system, most of the synchronization scheme do not give a systematic procedure to determine the response system and the drive signal. As a consequence, these schemes are closely related to the given

*Corresponding author.

drive system and could not be easily generalized to a class of chaotic systems. Unlike these methods, in this Letter a systematic procedure for synchronizing different classes of hyperchaotic systems is illustrated. By extending the results in Ref. 4, the approach can be applied to dynamic systems with one or more nonlinear elements as well as to time delay systems. If a structural property related to the drive equation is satisfied, then the response system is chosen in the *observer* form[2,4] and the synchronizing signal is designed so that the error system is globally asymptotically stabilized at the origin. In order to show that synchronization can be systematically achieved for different classes of hyperchaotic systems, the technique is applied to a recent example of 8th order circuit with a single nonlinear element,[7] to a cell equation in delayed Cellular Neural Networks[8] and to a 15-dimensional system with five nonlinear elements.[9] Simulation results are reported to show advantages and performances of the technique. In particular, synchronization in the presence of parameter mismatches and noise is analyzed.

2. Observer for Synchronizing Hyperchaos

The proposed procedure, which is based on five steps, is summarized in Sec. 2.1, whereas theoretical aspects and advantages of the method are illustrated in Sec. 2.2.

2.1. *Systematic procedure*

Step 1: Consider a drive system as hyperchaotic system belonging to the class C_m, which is defined as a dynamic system described by the following state equation:

$$\dot{\boldsymbol{x}}(t) = \boldsymbol{A}\boldsymbol{x}(t) + \boldsymbol{B}\boldsymbol{f}(\boldsymbol{x}(t-\tau)) + \boldsymbol{c}\,, \tag{1}$$

where $\boldsymbol{x} \in \Re^n$, $\boldsymbol{f} = (f_1(\boldsymbol{x}), f_2(\boldsymbol{x}), \ldots, f_m(\boldsymbol{x}))^T \in \Re^{m\times 1}$ with $f_i \neq f_j$ for $i \neq j$, $m \leq n$, $\boldsymbol{A} \in \Re^{n\times n}$ and $\boldsymbol{B} \in \Re^{n\times m}$ are known parameters whereas $\tau \in \Re^+$ is the delay.

Step 2: Consider the matrix:

$$\lfloor \boldsymbol{B} \quad \boldsymbol{AB} \quad \boldsymbol{A}^2\boldsymbol{B} \quad \cdots \quad \boldsymbol{A}^{n-1}\boldsymbol{B} \rfloor \tag{2}$$

and assume that Eq. (2) is full rank.

Step 3: Consider the matrix:

$$[\boldsymbol{A} - \boldsymbol{BK}] \tag{3}$$

and compute $\boldsymbol{K} \in \Re^{m\times n}$ so that the eigenvalues of Eq. (3) lie in the open left half plane.

Step 4: Let

$$\boldsymbol{y}(t) = \boldsymbol{f}(\boldsymbol{x}(t-\tau)) + \boldsymbol{K}\boldsymbol{x}(t) \tag{4}$$

be the output equation of the hyperchaotic system (1). Namely, Eq. (4) represents the synchronizing signal, which has been properly designed to feed the response system.

Step 5: Consider the response system:

$$\dot{\hat{\boldsymbol{x}}}(t) = \boldsymbol{A}\hat{\boldsymbol{x}}(t) + \boldsymbol{B}(\boldsymbol{y}(t) - \boldsymbol{K}\hat{\boldsymbol{x}}(t)) + \boldsymbol{c}\,. \tag{5}$$

The dynamic system (5) is a *global observer*[4] for the state of system (1), since the synchronization error system $\boldsymbol{e}(t) = (\hat{\boldsymbol{x}}(t) - \boldsymbol{x}(t))$ has a globally asymptotically stable equilibrium point for $\boldsymbol{e} = \mathbf{0}$, that is, $\boldsymbol{e}(t) \to \mathbf{0}$ as $t \to \infty$ for any initial condition $\hat{\boldsymbol{x}}(0)$, $\boldsymbol{x}(0)$.

2.2. *Discussion*

Five remarks are reported, with the aim of illustrating the theoretical aspect of each step.

Remark 1. Equation (1) can describe dynamic systems with one or more nonlinear elements as well as time delay systems. In particular, a system is said to belong to the class C_m if it contains m independent nonlinear elements. By considering C_1 (i.e., the class characterized by a *single* nonlinear element) and $\tau = 0$, it is easy to show that this class includes several well-known hyperchaotic systems, such as Rössler's system,[4] the Matsumoto–Chua–Kobayashi circuit[10] and its modified version,[11] the oscillators in Ref. 5, the circuit with hysteretic nonlinearity in Ref. 12 and the 8th order circuit proposed in Ref. 7. Referring to time delay systems belonging to C_1, this class includes the cell equation in delayed Cellular Neural Networks[8] and the oscillator implementing the Mackey–Glass mathematical model in Ref. 13. Finally, referring to higher classes of hyperchaotic systems (with $\tau = 0$), the class C_2 includes the coupled Chua's circuit in Ref. 14 and the circuit proposed by Carroll and Pecora in Ref. 15, whereas the coupled Lorenz systems in Ref. 16 and the coupled Chua's circuits forming a ring in Ref. 9 belong to the classes C_4 and C_5, respectively.

Remark 2. The assumption that Eq. (2) is full rank is not a restrictive condition. In fact, for all the systems mentioned in Remark 1 it can be easily verified that Eq. (2) is full rank. This clearly highlights the strength of the proposed approach.

Remark 3. By considering the drive system (1), the transmitted signal (4) and the response system (5), it is possible to derive the following linear time-invariant error system:

$$\dot{\boldsymbol{e}}(t) = \boldsymbol{A}\boldsymbol{e}(t) - \boldsymbol{B}\boldsymbol{K}\boldsymbol{e}(t) = \boldsymbol{A}\boldsymbol{e}(t) + \boldsymbol{B}\boldsymbol{u}(t)\,, \tag{6}$$

where $\boldsymbol{u}(t) = -\boldsymbol{K}\boldsymbol{e}(t) \in \Re^{m\times 1}$ plays the role of a state feedback. According to Step 2, if Eq. (2) is full rank, system (6) is controllable,[17] that is, its eigenvalues can be placed anywhere by proper state feedback. Therefore, by computing $\boldsymbol{K}$ so that the eigenvalues of Eq. (3) lie in the open left half plane, system (6) is globally asymptotically stabilized at the origin. On the other hand, if Eq. (2) is not full rank, system (6) can be transformed to the Kalman controllable canonical form[17] by means of a coordinate transformation $\boldsymbol{e} = \boldsymbol{T}\,\overline{\boldsymbol{e}} = [\boldsymbol{T}_1 \quad \boldsymbol{T}_2]\overline{\boldsymbol{e}}$:

$$\begin{bmatrix} \dot{\overline{\boldsymbol{e}}}_c \\ \dot{\overline{\boldsymbol{e}}}_{nc} \end{bmatrix} = \begin{bmatrix} \boldsymbol{T}_1^T & \boldsymbol{A}\boldsymbol{T}_1 & \boldsymbol{T}_1^T & \boldsymbol{A}\boldsymbol{T}_2 \\ & \boldsymbol{0} & \boldsymbol{T}_2^T & \boldsymbol{A}\boldsymbol{T}_2 \end{bmatrix} \begin{bmatrix} \overline{\boldsymbol{e}}_c \\ \overline{\boldsymbol{e}}_{nc} \end{bmatrix} + \begin{bmatrix} \boldsymbol{T}_1^T\ \boldsymbol{B} \\ \boldsymbol{0} \end{bmatrix} \boldsymbol{u}$$

$$= \begin{bmatrix} \overline{\boldsymbol{A}}_c & \overline{\boldsymbol{A}}_{12} \\ \boldsymbol{0} & \overline{\boldsymbol{A}}_{nc} \end{bmatrix} \begin{bmatrix} \overline{\boldsymbol{e}}_c \\ \overline{\boldsymbol{e}}_{nc} \end{bmatrix} + \begin{bmatrix} \overline{\boldsymbol{B}}_c \\ \boldsymbol{0} \end{bmatrix} \boldsymbol{u}\,, \tag{7}$$

where the eigenvalues of $\overline{\boldsymbol{A}}_c$ are controllable (i.e., they can be placed anywhere by $\boldsymbol{u} = -\boldsymbol{K}\boldsymbol{e}$), whereas the eigenvalues of $\overline{\boldsymbol{A}}_{nc}$ are uncontrollable (i.e., they are not affected by the introduction of any state feedback). Therefore, a necessary and sufficient condition for the existence of a matrix $\boldsymbol{K}$ able to stabilize system (6) is that the eigenvalues of $\overline{\boldsymbol{A}}_{nc}$ have negative real parts. It can be concluded that the approach works even if Eq. (2) is not full rank, provided that the uncontrollable eigenvalues lie in the open left half plane.

Remark 4. For systems belonging to class C_1 Eq. (4) represents a *scalar* synchronizing signal. Roughly speaking, it can be obtained by adding the current in the nonlinear device to a linear combination of the circuit state variables. Although in this paper the attention is not focused on hardware implementation issues, it is worth noting that such signals are not difficult to be realized. For instance, in Ref. 18 it is shown that scalar synchronizing signals can be implemented using operational amplifier configurations, which consist of buffers, inverting amplifiers, current-to-voltage converters and summers.

Remark 5. By taking into account that Eq. (6) is globally asymptotically stabilized at the origin, it is clear that Eq. (5) behaves as a global observer[4,17] for the state of the drive system (1). This means that, for any initial condition $\hat{\boldsymbol{x}}(0)$, the state of the observer $\hat{\boldsymbol{x}}(t)$ converges to the state of the plant $\boldsymbol{x}(t)$.

The proposed technique has several advantages:

(i) it is rigorous (since synchronization is *proved* using results from linear system theory[17]);
(ii) it does not require either the computation of the Lyapunov exponents or initial conditions of drive and response systems belonging to the same basin of attraction;
(iii) it extends the results in Ref. 4 to time delay systems;
(iv) it enables systems with one or more nonlinear elements to be synchronized (instead of systems with a single nonlinear term, as in Ref. 4);
(v) it is simpler that the approach in Ref. 4, due to the adoption of *linear* observers (instead of *nonlinear* ones).

3. Systems Belonging to the Class C_1: Synchronization Examples

Herein, two examples of hyperchaotic systems belonging to the class C_1 are synchronized. In particular, in the first example 8th order circuits are considered and robustness of synchronization with respect to parameter mismatches is analyzed. In the second example cell equations in delayed Cellular Neural Networks are considered and robustness of synchronization in the presence of significant amount of noise is discussed.

3.1. *Synchronization of 8th order oscillators*

The high-order circuit family recently proposed in Ref. 7 contains a novel two-terminal device, called chaos-diode (χ-diode), which includes both a negative impedance converter and the Schmitt trigger. An example of 8th order circuit is reported in Fig. 1. Simulation and experimental results have confirmed the hyperchaotic behavior of this oscillator, which is characterized by six positive Lyapunov exponents.[7] The projection of the hyperchaotic attractor on the plane (x_1, x_2) is reported in Fig. 2.

By applying the tool with $\tau = 0$ and by considering the circuit parameters reported in Ref. 7, the state equations of the oscillator can be written in dimensionless form as:

$$\begin{bmatrix} \dot{x}_1 \\ \dot{x}_2 \\ \dot{x}_3 \\ \dot{x}_4 \\ \dot{x}_5 \\ \dot{x}_6 \\ \dot{x}_7 \\ \dot{x}_8 \end{bmatrix} = \begin{bmatrix} 0.6 & -1 & 0 & -1 & 0 & -1 & 0 & -1 \\ 1 & 0 & 0 & 0 & 0 & 0 & 0 & 0 \\ 0 & 0 & 0 & 1 & 0 & 1 & 0 & 1 \\ 1 & 0 & -1 & 0 & 0 & 0 & 0 & 0 \\ 0 & 0 & 0 & 0 & 0 & 1 & 0 & 1 \\ 1 & 0 & -1 & 0 & -1 & 0 & 0 & 0 \\ 0 & 0 & 0 & 0 & 0 & 0 & 0 & 1 \\ 1 & 0 & -1 & 0 & -1 & 0 & -1 & 0 \end{bmatrix} \begin{bmatrix} x_1 \\ x_2 \\ x_3 \\ x_4 \\ x_5 \\ x_6 \\ x_7 \\ x_8 \end{bmatrix} + \begin{bmatrix} -4.2 \\ 0 \\ 0 \\ 0 \\ 0 \\ 0 \\ 0 \\ 0 \end{bmatrix} s_j(x_1, s_{j-1}), \quad (8)$$

where $s_j = H(x_1 - 1 + 0.9s_{j-1})$, $j = 1, 2, \ldots$, is the discrete state function that describes the hysteretic action of the Schmitt trigger. This function, which depends on the variable x_1 as well as on the previous state s_{j-1}, alternates between 1 and 0, since $H(u) = 0$ if $u < 0$ and $H(u) = 1$ if $u \geq 0$.

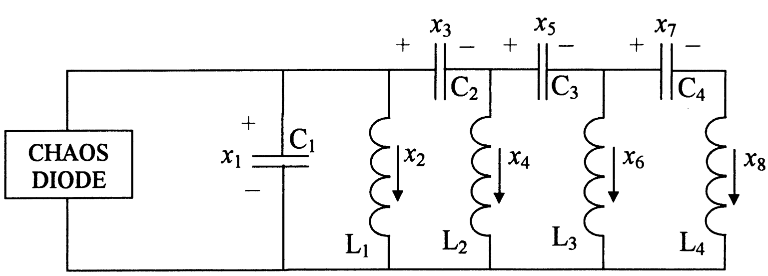

Fig. 1. The 8th order circuit described by Eq. (8).

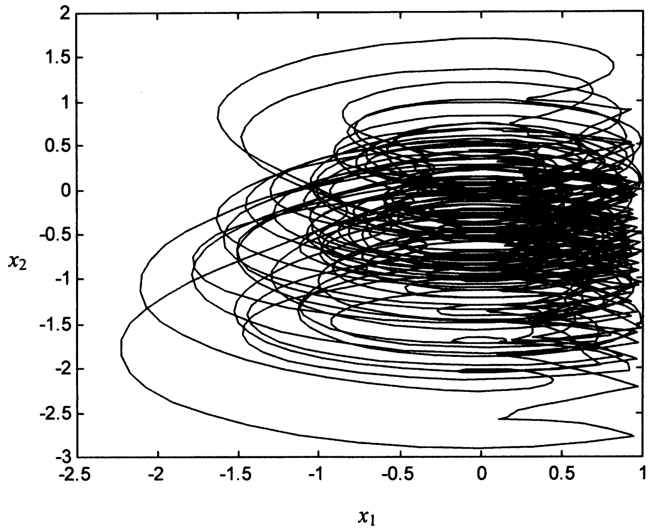

Fig. 2. The projection of the hyperchaotic attractor of system (8) on the plane (x_1, x_2).

By considering Step 2, it can be easily shown that Eq. (2) is full rank. Therefore, according to Step 3, the eigenvalues of Eq. (3) can be placed in the open left half plane by suitable $\boldsymbol{K}$. By placing them in -1, it results $\boldsymbol{K} = [-2.0476 \quad 0 \quad 0 \quad -5.0000 \quad -3.8095 \quad 1.9048 \quad 5.7143 \quad -1.1905]$, which gives the following *scalar* transmitted signal:

$$y(t) = s_j(x_1, s_{j-1}) + \sum_{i=1}^{8} K_i x_i(t)\,. \tag{9}$$

Finally, according to Step 5, the response system in the observer form is:

$$\begin{bmatrix} \dot{\hat{x}}_1 \\ \dot{\hat{x}}_2 \\ \dot{\hat{x}}_3 \\ \dot{\hat{x}}_4 \\ \dot{\hat{x}}_5 \\ \dot{\hat{x}}_6 \\ \dot{\hat{x}}_7 \\ \dot{\hat{x}}_8 \end{bmatrix} = \begin{bmatrix} 0.6 & -1 & 0 & -1 & 0 & -1 & 0 & -1 \\ 1 & 0 & 0 & 0 & 0 & 0 & 0 & 0 \\ 0 & 0 & 0 & 1 & 0 & 1 & 0 & 1 \\ 1 & 0 & -1 & 0 & 0 & 0 & 0 & 0 \\ 0 & 0 & 0 & 0 & 0 & 1 & 0 & 1 \\ 1 & 0 & -1 & 0 & -1 & 0 & 0 & 0 \\ 0 & 0 & 0 & 0 & 0 & 0 & 0 & 1 \\ 1 & 0 & -1 & 0 & -1 & 0 & -1 & 0 \end{bmatrix} \begin{bmatrix} \hat{x}_1 \\ \hat{x}_2 \\ \hat{x}_3 \\ \hat{x}_4 \\ \hat{x}_5 \\ \hat{x}_6 \\ \hat{x}_7 \\ \hat{x}_8 \end{bmatrix} + \begin{bmatrix} -4.2 \\ 0 \\ 0 \\ 0 \\ 0 \\ 0 \\ 0 \\ 0 \end{bmatrix} \left(y(t) - \sum_{i=1}^{8} K_i \hat{x}_i(t) \right). \tag{10}$$

In order to show the effectiveness of the proposed synchronization technique, robustness with respect to parameter mismatches is analyzed. For instance, suppose that the value of the inductance L_4 in the response system is different from the corresponding value in the drive system. By considering Eq. (10), this means that the elements (different from zero) in the last row of $\boldsymbol{A}$ are different from the corresponding elements in Eq. (8). Suppose that the mismatch is 10% (notice that tolerances usually are 5% for electronic devices). The synchronization between the variables x_1 and $\hat{x}_1$ is shown in Fig. 3(a) whereas the error $e = \hat{x}_1 - x_1$, due to the mismatch, is reported in Fig. 3(b). This figure highlights that the synchronization property is preserved in the presence of single parameter mismatch. Finally, the robustness with respect to mismatches of all the parameters is analyzed. Suppose that the values of the circuit parameters of the response system are all different from the corresponding values of the drive system. By considering Eq. (10), this means that all the elements (different from zero) in $\boldsymbol{A}$ are different from the corresponding elements in Eq. (8). Suppose that the mismatch for all the parameters is 10%. The time waveforms of x_1 and $\hat{x}_1$ are shown in Fig. 4(a) whereas the error $e = \hat{x}_1 - x_1$ is reported in Fig. 4(b). Although the error is larger than before, Fig. 4(a) shows that the variable $\hat{x}_1$ is still able to track the driving signal x_1.

3.2. *Synchronization of cell equations in delayed Cellular Neural Networks*

Time-delay systems have an infinite-dimensional state space. They can generate very complex chaotic behaviors, characterized by an arbitrary large number of positive Lyapunov exponents. The system considered herein is the cell equation in Cellular Neural Networks with delay.[8] By introducing dimensionless variables x

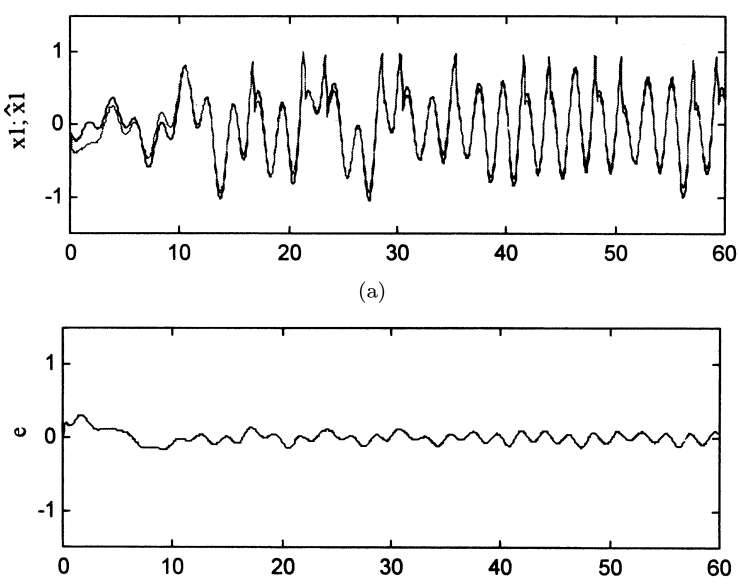

Fig. 3. Synchronization of 8th order oscillators in the presence of single parameter mismatch: (a) time waveforms of chaotic signals x_1 and $\hat{x}_1$; (b) time waveform of the error $e = \hat{x}_1 - x_1$.

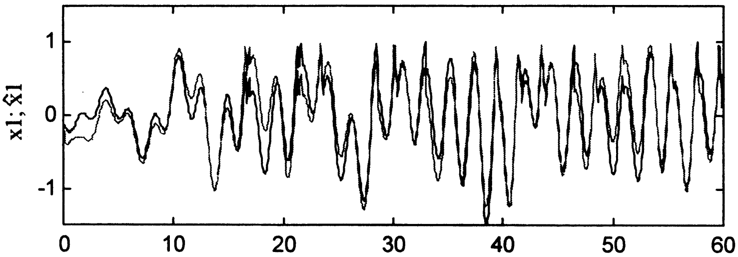

(a)

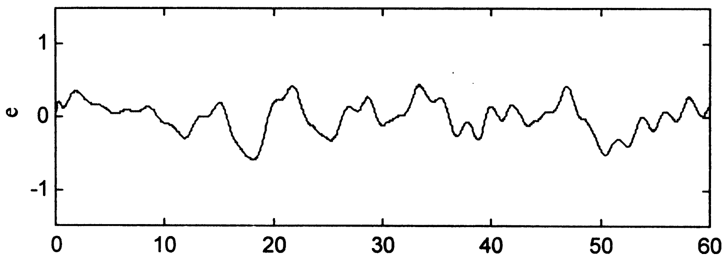

(b)

Fig. 4. Synchronization of 8th order oscillators in the presence of mismatches of all the parameters: (a) time waveforms of chaotic signals x_1 and $\hat{x}_1$; (b) time waveform of the error $e = \hat{x}_1 - x_1$.

and t as well as dimensionless delay τ, the drive system can be described by[8]:

$$\dot{x}(t) = 0.001x(t) - 1.9\left[2\left(|x_\tau + 1| - |x_\tau - 1|\right) - 1.5\left(\left|x_\tau + \frac{4}{3}\right| - \left|x_\tau - \frac{4}{3}\right|\right)\right], \quad (11)$$

where $x_\tau = x(t - \tau)$. A detailed analysis of the complex dynamics generated by piecewise-linear equations in Eq. (11) is reported in Ref. 8. For the parameter values considered herein, the chaotic attractor on the plane $(x(t),\, x(t-\tau))$ is illustrated in Fig. 5. According to Steps 2 and 3, matrix (3) turns into the eigenvalue $(a - bK)$, which can be placed in the open left half plane for $K < -0.001/1.9$. By choosing $K = -1$, Step 4 gives the following scalar transmitted signal:

$$y(t) = -x(t) + \left[2(|x_\tau + 1| - |x_\tau - 1|) - 1.5\left(\left|x_\tau + \frac{4}{3}\right| - \left|x_\tau - \frac{4}{3}\right|\right)\right]. \quad (12)$$

Therefore, according to Step 5, the response system in the observer form is:

$$\dot{\hat{x}}(t) = 0.001\hat{x}(t) - 1.9(y(t) + \hat{x}(t))\,, \quad (13)$$

where $y(t)$ represents both the transmitted and the received signal, since the systems to be synchronized have been connected to each other through an ideal channel.

Now, the properties of synchronization in the presence of noise are investigated. Suppose that the circuits to be synchronized are connected to each other by coaxial cable. By considering optimal passive equalization of the cable, the output of the

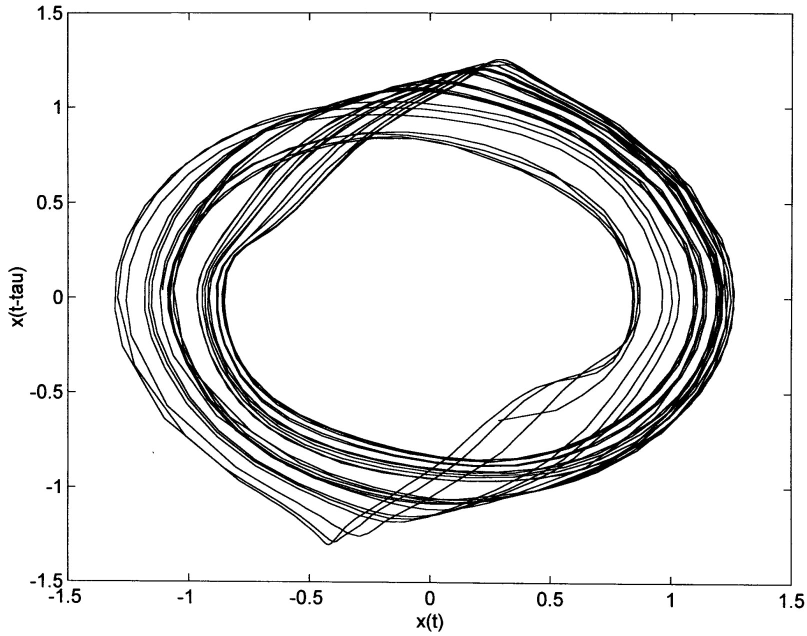

Fig. 5. The hyperchaotic attractor of system (11) displayed on the plane $(x(t), x(t-\tau))$ for $\tau = 1$.

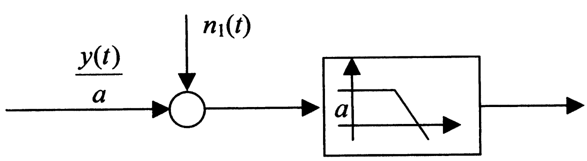

Fig. 6. Low-pass filter at the response system in the presence of noisy channel: block diagram.

equalizer can be described by:

$$\frac{y(t)}{a} + n_1(t)\,, \tag{14}$$

where a is the channel attenuation whereas $n_1(t)$ represents Gaussian noise with zero mean and fixed variance. Two different synchronization cases are now analyzed: in the first case simple gain a is considered at the response system, whereas in the second case a low-pass filter is designed, with the aim of filtering out the noise (see Fig. 6). In the case of simple gain a, the synchronizing signal is given by:

$$a\left(\frac{y(t)}{a} + n_1(t)\right) = y(t) + n(t)\,, \tag{15}$$

where $n(t) = an_1(t)$. As a consequence, the response system (13) assumes the form:

$$\dot{\hat{x}}(t) = 0.001\hat{x}(t) - 1.9(y_{\mathrm{amp}}(t) + \hat{x}(t))\,, \tag{16}$$

where $y_{\mathrm{amp}}(t)$ is the amplified signal (15). Numerical simulations of systems (16) and (11) are carried out by considering increasing levels of noise $n(t)$ added to the transmitted signal $y(t)$. In particular, starting from the top to the bottom, Fig. 7 shows the synchronization between $x(t)$ and $\hat{x}(t)$ for $n \sim N(0, 0.1^2)$, $n \sim N(0, 0.3^2)$ and $n \sim N(0, 0.5^2)$. For all the cases the figure highlights that the observer variable $\hat{x}(t)$ is able to track the driving variable $x(t)$. Additionally, Fig. 8 shows the synchronization for an increased level of noise, that is, $n \sim N(0, 0.7^2)$. The figure highlights that $\hat{x}(t)$ is still able to track $x(t)$, even though in this case the amplitude of noise $n(t)$ can be considerably greater (in some instant) than the amplitude of the transmitted signal $y(t)$ (see Fig. 9).

In order to enhance the performances of the synchronization scheme, a low-pass filter is now designed. By considering the plot of the average power spectral density of the transmitted signal $y(t)$ (see Fig. 10), it can be argued that most of the significant frequencies are less than 4 (dimensionless units). By choosing a first-order low-pass filter with cut-off frequency equal to 4, its transfer function is described by:

$$\frac{a}{0.25s + 1}. \tag{17}$$

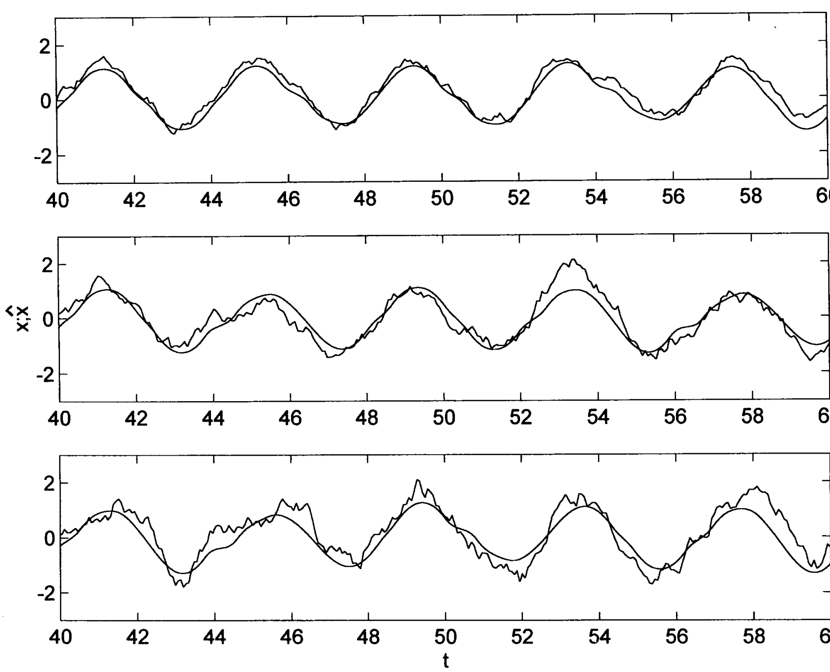

Fig. 7. From the top to the bottom, synchronization of delayed cell equations (11) and (16) in the presence of noisy channel with $n \sim N(0, 0.1^2)$, $n \sim N(0, 0.3^2)$ and $n \sim N(0, 0.5^2)$. Chaotic signals x and $\hat{x}$ are plotted for large t.

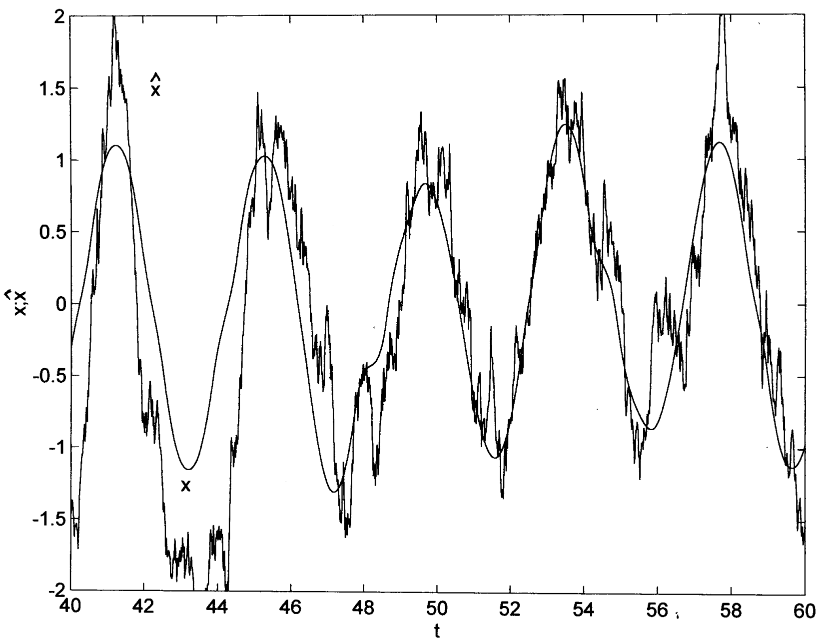

Fig. 8. Synchronization of delayed cell equations (11) and (16) in the presence of noisy channel with $n \sim N(0, 0.7^2)$. Notice that simple amplifier with gain a has been used.

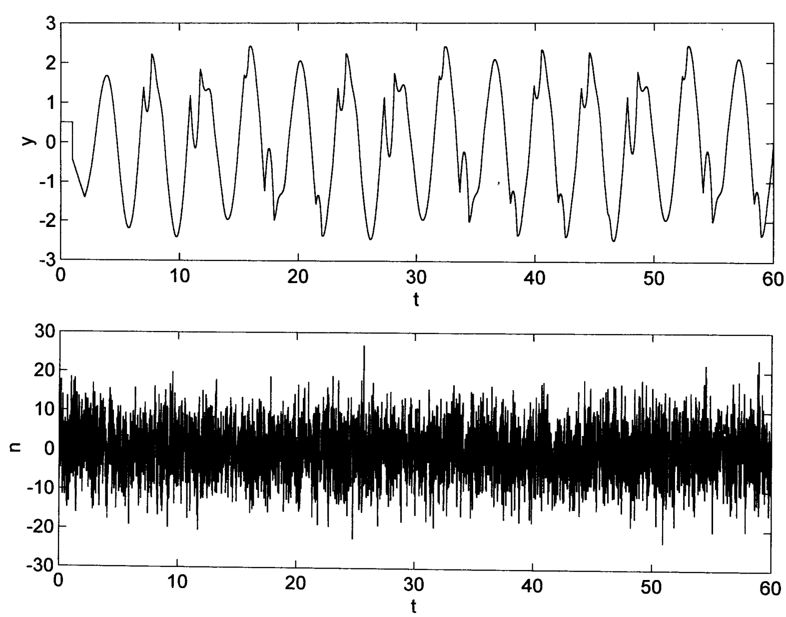

Fig. 9. Time waveforms of transmitted signal $y(t)$ (top) and of noise $n(t)$ with $n \sim N(0, 0.7^2)$ (bottom).

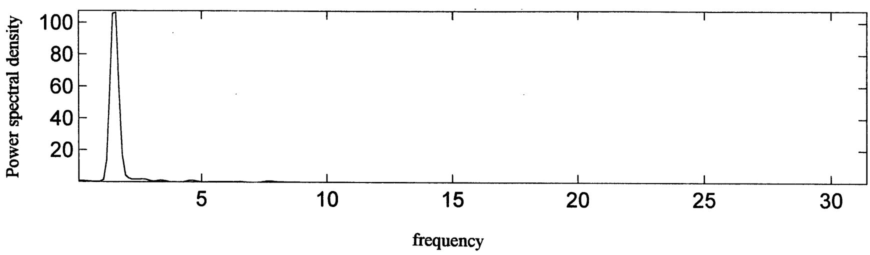

Fig. 10. Average power spectral density of transmitted signal $y(t)$.

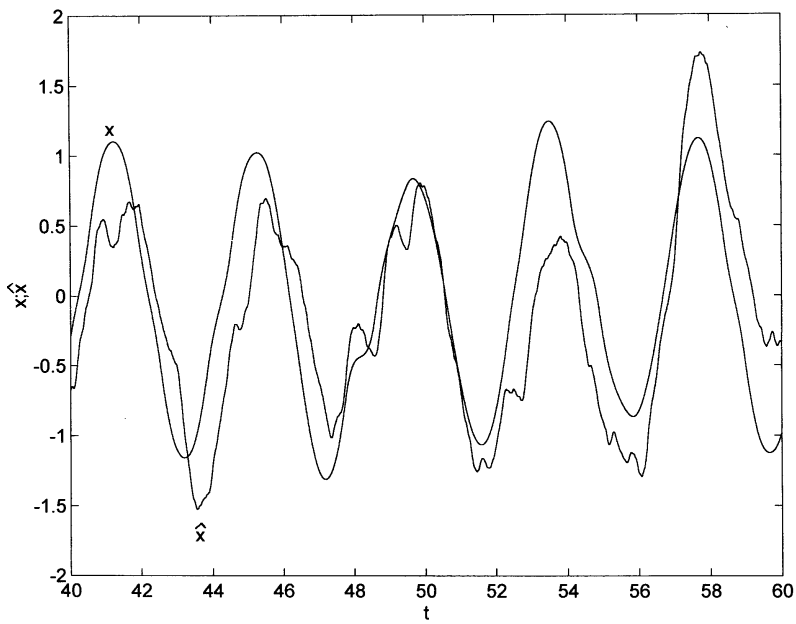

Fig. 11. Synchronization of delayed cell equations (11) and (18) in the presence of noisy channel with $n \sim N(0, 0.7^2)$. Notice that low-pass filter (17) has been used.

By indicating the output of the low-pass filter as $y_{\text{fil}}(t)$, the response system (13) assumes the form:

$$\dot{\hat{x}}(t) = 0.001\hat{x}(t) - 1.9(y_{\text{fil}}(t) + \hat{x}(t)) . \tag{18}$$

Numerical simulations of systems (18) and (11) are carried out by considering $n \sim N(0, 0.7^2)$. In particular, synchronization between $x(t)$ and $\hat{x}(t)$ is illustrated in Fig. 11. The comparison between Figs. 8 and 11 clearly highlights the improvements of variable $\hat{x}(t)$ in tracking variable $x(t)$, owing to filtering of noisy synchronizing signal.

Remark 6. We would stress that the analysis developed in the previous example has not been made for communications applications. The aim of the example was to investigate the synchronization properties in the presence of noisy channel and filtered signals.

4. Systems Belonging to Higher Classes: Synchronization Example

In this section a 15-dimensional system is considered, which consists of five identical coupled Chua's circuits forming a ring.[9] For this system experimental observation of hyperchaos has been reported in Ref. 9. The parameters of the drive system (1), which belongs to the class C_5 with $\tau = 0$, are the following:

$$\boldsymbol{A} = \begin{bmatrix} \boldsymbol{A}_1 & \boldsymbol{A}_2 & \boldsymbol{0} & \boldsymbol{0} & \boldsymbol{0} \\ \boldsymbol{0} & \boldsymbol{A}_1 & \boldsymbol{A}_2 & \boldsymbol{0} & \boldsymbol{0} \\ \boldsymbol{0} & \boldsymbol{0} & \boldsymbol{A}_1 & \boldsymbol{A}_2 & \boldsymbol{0} \\ \boldsymbol{0} & \boldsymbol{0} & \boldsymbol{0} & \boldsymbol{A}_1 & \boldsymbol{A}_2 \\ \boldsymbol{A}_2 & \boldsymbol{0} & \boldsymbol{0} & \boldsymbol{0} & \boldsymbol{A}_1 \end{bmatrix}, \quad \boldsymbol{A}_1 = \begin{bmatrix} -3.2 & 10 & 0 \\ 1 & -1.01 & 1 \\ 0 & -14.87 & 0 \end{bmatrix},$$

$$\boldsymbol{A}_2 = \begin{bmatrix} 0 & 0 & 0 \\ 0 & 0.01 & 0 \\ 0 & 0 & 0 \end{bmatrix}, \quad \boldsymbol{0} \in \Re^{3\times 3}, \tag{19}$$

$$\boldsymbol{B} = \begin{bmatrix} \boldsymbol{b} & \boldsymbol{0} & \boldsymbol{0} & \boldsymbol{0} & \boldsymbol{0} \\ \boldsymbol{0} & \boldsymbol{b} & \boldsymbol{0} & \boldsymbol{0} & \boldsymbol{0} \\ \boldsymbol{0} & \boldsymbol{0} & \boldsymbol{b} & \boldsymbol{0} & \boldsymbol{0} \\ \boldsymbol{0} & \boldsymbol{0} & \boldsymbol{0} & \boldsymbol{b} & \boldsymbol{0} \\ \boldsymbol{0} & \boldsymbol{0} & \boldsymbol{0} & \boldsymbol{0} & \boldsymbol{b} \end{bmatrix}, \quad \boldsymbol{b} = \begin{bmatrix} 2.95 \\ 0 \\ 0 \end{bmatrix}, \quad \boldsymbol{0} \in \Re^{3\times 1}, \ \boldsymbol{c} = \boldsymbol{0} \in \Re^{15\times 1}, \tag{20}$$

$$\begin{aligned} \boldsymbol{f}(\boldsymbol{x}) &= \begin{bmatrix} f(x_1) & f(x_4) & f(x_7) & f(x_{10}) & f(x_{13}) \end{bmatrix}^T, \\ f(x_i) &= |x_i + 1| - |x_i - 1|\,. \end{aligned} \tag{21}$$

The projection of the hyperchaotic attractor on (x_1, x_2, x_4) is reported in Fig. 12. According to Steps 2 and 3, since $\lfloor \boldsymbol{B} \ \ \boldsymbol{AB} \ \ \boldsymbol{A}^2\boldsymbol{B} \ \ \cdots \ \ \boldsymbol{A}^{14}\boldsymbol{B} \rfloor$ is full rank it is possible to place the error system eigenvalues in $\{-1, -1, -1, -1, -1, -2, -2, -2, -2, -2, -3, -3, -3, -3, -3\}$ by using the gain matrix:

$$\boldsymbol{K} = \begin{bmatrix} \boldsymbol{K}_1 & \boldsymbol{K}_2 & \boldsymbol{0} & \boldsymbol{0} & \boldsymbol{0} \\ \boldsymbol{0} & \boldsymbol{K}_1 & \boldsymbol{K}_2 & \boldsymbol{0} & \boldsymbol{0} \\ \boldsymbol{0} & \boldsymbol{0} & \boldsymbol{K}_1 & \boldsymbol{K}_2 & \boldsymbol{0} \\ \boldsymbol{0} & \boldsymbol{0} & \boldsymbol{0} & \boldsymbol{K}_1 & \boldsymbol{K}_2 \\ \boldsymbol{K}_2 & \boldsymbol{0} & \boldsymbol{0} & \boldsymbol{0} & \boldsymbol{K}_1 \end{bmatrix} \in \Re^{5\times 15}, \tag{22}$$

where $\boldsymbol{K}_1 = [0.6068 \ \ 0.3695 \ \ 1.5547]$, $\boldsymbol{K}_2 = [0.0034 \ \ 0.0135 \ \ 0.0034]$ and $\boldsymbol{0} \in \Re^{1\times 3}$. Thus, by considering the five-dimensional synchronizing signal given by:

$$\boldsymbol{y}(t) = \boldsymbol{f}(\boldsymbol{x}(t)) + \boldsymbol{K}\boldsymbol{x}(t)\,, \tag{23}$$

it is easy to show that observer (5) behaves so that $\hat{\boldsymbol{x}} \to \boldsymbol{x}$ as $t \to \infty$ for each initial state $\hat{\boldsymbol{x}}(0)$, that is, initial conditions of drive and response systems need not to belong to the same basin of attraction.

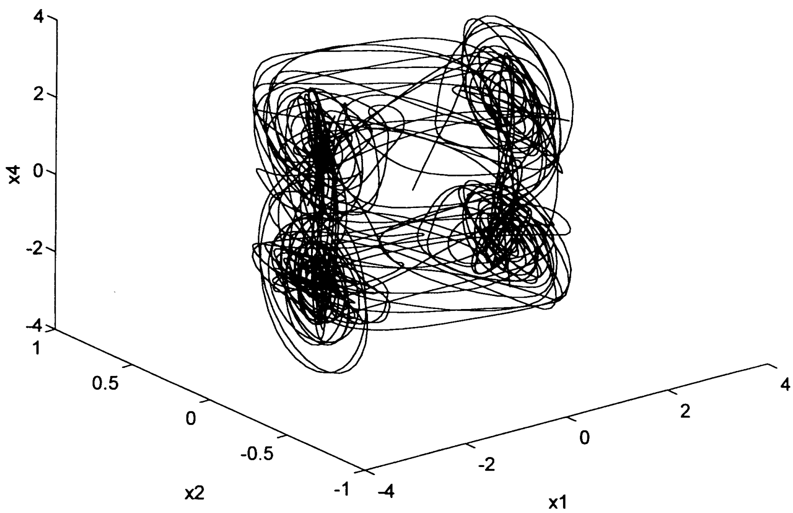

Fig. 12. The projection on (x_1, x_2, x_4) of the hyperchaotic attractor obtained from Eqs. (19)–(21).

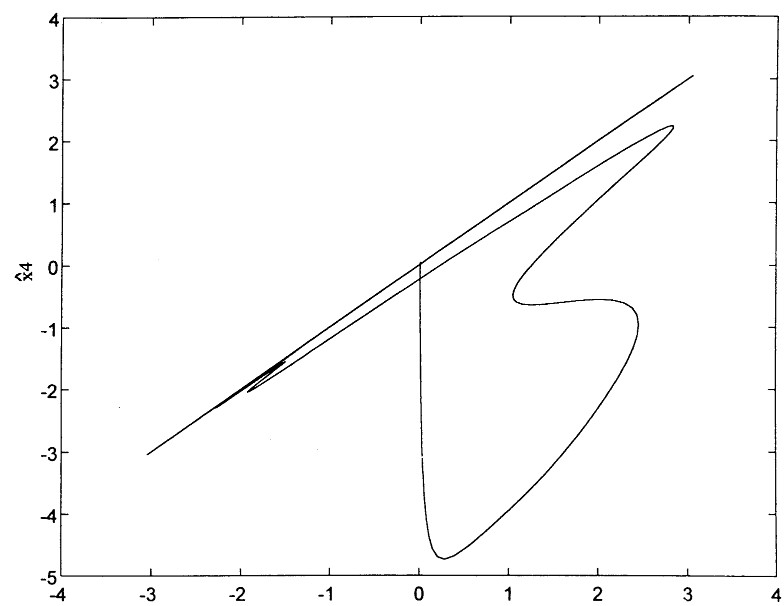

Fig. 13. System belonging to class C_5: synchronization between the variables x_4 and $\hat{x}_4$.

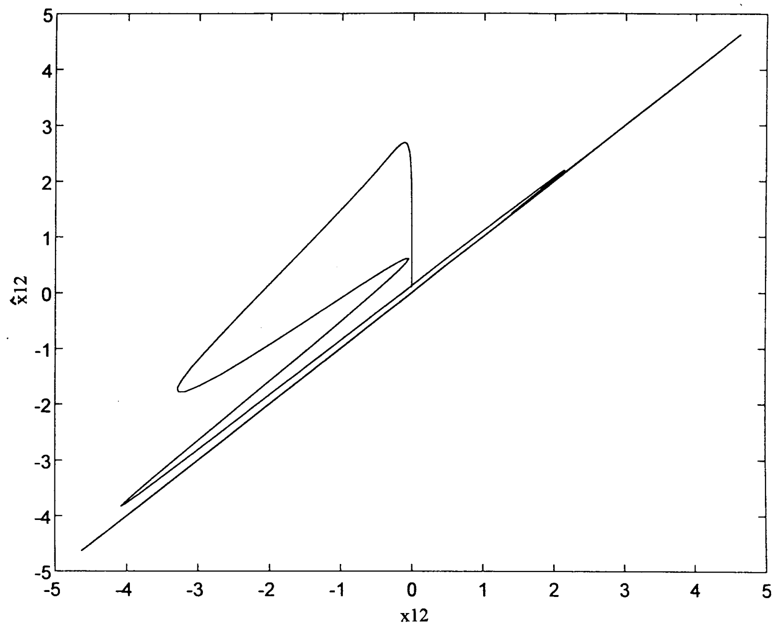

Fig. 14. System belonging to class C_5: synchronization between the variables x_{12} and $\hat{x}_{12}$.

Simulation results have confirmed this property. Namely, synchronization between the variables $(x_4, \hat{x}_4)$ and $(x_{12}, \hat{x}_{12})$ is illustrated in Figs. 13 and 14, respectively. These figures clearly show that synchronization is achieved after a certain transient time, which depends on the initial state of the response system.

5. Conclusion

In this Letter a systematic tool for synchronizing hyperchaos has been illustrated. The method, based on five steps, can be applied to dynamic systems with one or more nonlinear elements as well as to time delay systems. The technique exploits linear observer as response system and is based on a structural property related to the drive equation. The tool has been applied to a recent example of 8th order oscillator, to a cell equation in delayed neural networks and to an example of 15-dimensional system, which consists of five identical coupled Chua's circuits. Finally, synchronization properties in the presence of parameter mismatches, noisy channel and filtered signals have been numerically investigated.

References

1. T. L. Carroll and L. M. Pecora, "Synchronizing chaotic circuits", *IEEE Trans. CAS* **38** (1991) 453–456.
2. H. Nijmeijer and I. M. Y. Mareels, "An observer looks at synchronization", *IEEE Trans. CAS* **44** (1997) 882–890.

3. J. H. Peng, E. J. Ding, M. Ding, and W. Yang, "Synchronizing hyperchaos with a scalar transmitted signal", *Phys. Rev. Lett.* **76** (1996) 904–907.
4. G. Grassi and S. Mascolo, "Nonlinear observer design to synchronize hyperchaotic systems via a scalar signal", *IEEE Trans. CAS* **44** (1997) 1011–1014.
5. G. Grassi and S. Mascolo, "Synchronization of hyperchaotic oscillators using a scalar signal", *IEE Electron. Lett.* **34** (1998) 424–425.
6. T. Yang and L. O. Chua, "Impulsive control and synchronization of nonlinear dynamical systems and application to secure communication", *Int. J. Bifur. Chaos* **7** (1997) 645–664.
7. E. Lindberg, A. Tamasevicius, A. Cenys, G. Mykolaitis, and A. Namajunas, "Hyperchaos via χ-diode", *Proc. 6th Int. Workshop on Nonlinear Dynamics of Electronic Systems* (*NDES 98*), Budapest (1998) 125–128.
8. H. Lu, Y. He, and Z. He, "A chaos generator: Analyses of complex dynamics of a cell equation in delayed Cellular Neural Networks", *IEEE Trans. CAS* **45** (1998) 178–181.
9. T. Kapitaniak, L. O. Chua, and G. Q. Zhong, "Experimental hyperchaos in coupled Chua's circuits", *IEEE Trans. CAS* **41** (1994) 499–503.
10. T. Matsumoto, L. O. Chua, and K. Kobayashi, "Hyperchaos: Laboratory experiment and numerical confirmation", *IEEE Trans. CAS* **33** (1986) 1143–1147.
11. A. Tamasevicius, "Hyperchaotic circuits: State of the art", in *Proc. Fifth Int. Workshop on Nonlinear Dynamics of Electronic Systems* (*NDES '97*), Moscow (1997) 97–102.
12. T. Saito, "An approach toward higher dimensional hysteresis chaos generators", *IEEE Trans. CAS* **37** (1990) 399–409.
13. A. Namajunas, K. Pyragas, and A. Tamasevicius, "An electronic analog of the Mackey–Glass system", *Phys. Lett. A* **201** (1995) 42–46.
14. V. S. Anishchenko, T. Kapitaniak, M. A. Safonova, and O. V. Sosnovzeva, "Birth of double–double scroll attractor in coupled Chua circuits", *Phys. Lett. A* **192** (1994) 207–214.
15. T. L. Carroll and L. M. Pecora, "A circuit for studying the synchronization of chaotic systems", *Int. J. Bifur. Chaos* **2** (1992) 659–667.
16. A. Stefanski, T. Kapitaniak, and J. Brindley, "Dynamics of coupled Lorenz systems and its geophysical implications", *Physica D* **98** (1996) 594–598.
17. T. Kailath, *Linear Systems*, Prentice Hall, New Jersey, 1980.
18. D. A. Miller and G. Grassi, "Experimental realization of observer-based hyperchaos synchronization", *IEEE Trans. CAS-I*, March 2001.